Implementation of Green's function molecular dynamics: an extension to LAMMPS

Ling Ti Kong, Guido Bartels, Carlos Campañá [1],
Colin Denniston [2], Martin H. Müser [2]

Department of Applied Mathematics, University of Western Ontario, London, Ontario, Canada N6A 5B7

Abstract

The Green's function molecular dynamics method, which enables one to study the elastic response of a three-dimensional solid to an external stress field by taking into consideration only the surface atoms, was implemented as an extension to an open source classical molecular dynamics simulation code LAMMPS. This was done in the style of fixes. The first fix, FixGFC, measures the elastic stiffness coefficients for a (small) solid block of a given material by making use of the fluctuation-dissipation theorem. With the help of the second fix, FixGFMD, the coefficients obtained from FixGFC can then be used to compute the elastic forces for a (large) block of the same material. Both fixes are designed to be run in parallel and to exploit the functions provided by LAMMPS.

PACS: 68.35.Ja, 46.55.+d, 02.70.Ns

Key words: Elastic stiffness coefficients; elastic Green's functions; semi-infinite solids; molecular dynamics

PROGRAM SUMMARY

---

[1] Now at: CANMET-Materials Technology Laboratory, Natural Resources Canada, Ottawa, Ontario, K1A 0G1, Canada
[2] Corresponding authors, e-mail: cdennist@uwo.ca, mmuser@uwo.ca

Nature of problem and solution method:
Using molecular dynamics to study elastically deforming solids imposes very high computational costs because portions of the solid far away from the interface or contact points need to be included in the simulation to reproduce the effects of long-range elastic deformations. Green's function molecular dynamics (GFMD) incorporates the full elastic response of semi-infinite solids so that only surface atoms have to be considered in molecular dynamics simulations, thus reducing the problem from three dimensions to two dimensions without compromising the physical essence of the problem.

Restrictions:
The mean equilibrium positions of the GFMD surface atoms must be in a plane and be periodic in the plane, so that the Born-von Karman boundary condition can be used. In addition, only deformation within the harmonic regime is expected in the surface layer during Green's function molecular dynamics.

Running time:
FixGFC varies from minutes to days, depending on the system size, the numbers of processors used, and the complexity of the force field.
FixGFMD varies from seconds to days depending on the system size and numbers of processors used.

References:

[1] C. Campañá and M. H. Müser, Phys. Rev. B **74**, 075420 (2006).

LONG WRITE-UP

1 Introduction

Many physical processes that are commonly associated with an interface of an elastic solid can be strongly affected by long-range elastic deformation in the bulk of the solid. Examples include the contact mechanics or friction between elastically deformable bodies with rough surfaces [1–5]. In order to properly include the effect of long-range elastic deformation with molecular dynamics (MD) or related atomistic simulation techniques, it is typically necessary to have the linear size normal to the interface be as large as the largest length scale on which roughness can be found. In simulations, this is typically the linear lateral (direction parallel to the interface) size L of the interface. An all-atom simulation of such large blocks would require significant computing time and memory, frequently making it unfeasible to study systems of meaningful size.

Green's function molecular dynamics (GFMD) [4] is a method that can reduce the computational cost significantly while remaining numerically accurate. The main idea behind GFMD is that all internal (harmonic) modes of an elastic body can be integrated out leading to effective interactions of those atoms whose degrees of freedom couple to an external force [6]. That is to say, one calculates renormalized interactions between surface atoms. Thus the full elastic response of semi-infinite solids is incorporated so that only the surface atoms have to be considered in molecular dynamics simulations.

We describe in this paper the physical background of Green's function molecular dynamics and present an implementation into a classic molecular dynamics simulation code LAMMPS [7–9], which is done in the style of fixes. In LAMMPS, a "fix" is any operation that is computed during a time step which alters some property of the system. Essentially everything that happens during a simulation besides potential force computation, neighbor list construction, and some forms of output, is a "fix" [9]. Our first fix, FixGFC, measures the elastic Green's functions, from which elastic stiffness coefficients are calculated by making use of the fluctuation-dissipation theorem. FixGFC is called at the end of each N'th time step (N to be specified by user) after equilibration has occurred. Our second fix, FixGFMD, first reads in the output produced in a previous run using FixGFC and then extrapolates the data to the appropriate system size during the initialization. It then computes the elastic forces inside an elastic manifold during each time step. FixGFMD is called after the computation of all other forces. As an alternative to reading in the elastic stiffness coefficients, FixGFMD can also make use of analytical solutions for simple cubic lattices with given spring couplings [10,11].

In the remaining part of this paper, the GFMD methodology and its implementation into LAMMPS are sketched. Some technical issues are highlighted, which were not addressed in the original literature [4]. We also present some applications which we used to test our implementation of the fixes into LAMMPS.

2 Theoretical background

In this section, the theoretical background behind GFMD will be reviewed. Some aspects of GFMD are presented in more detail in Ref. [4], in particular those pertaining to a sparse representation of the stiffness coefficients in the Brillouin zone. However, a more in depth derivation of the fluctuation-dissipation relation we used will be given here. New technical issues arose while implementing GFMD into LAMMPS and while extending the methodology from simple Bravais lattices to lattices with basis. Those issues will be discussed in the next section.

Consider a system of bi-linearly coupled (harmonic) displacements $\{u_i\}$, whose potential energy V is given by

$$V = \sum_{i,j} \frac{1}{2} \phi_{ij} u_i u_j, \tag{1}$$

where $\phi_{ij} = \phi_{ji}$. The Green's function coefficients are defined as the second moments of the displacements,

$$\mathbf{G}_{ij} = \beta \langle u_i u_j \rangle, \tag{2}$$

where $\beta = 1/k_B T$ and $\langle \cdots \rangle$ denotes the ensemble average. In thermal equilibrium, the distribution of $\{u_i\}$ will follow Boltzmann statistics. Thus the probability to find a given configuration $\{u_i\}$ will be proportional to $\exp(-\beta V)$ and

$$\mathbf{G}_{ij} = \frac{\beta}{Z(\beta)} \int du_1 \cdots du_N u_i u_j e^{-\beta V}, \tag{3}$$

where $Z(\beta) = \int du_1 \cdots du_N e^{-\beta V}$ is the partition function. By expressing u_i in terms of the eigenvectors of the $\mathbf{\Phi}$ matrix (the matrix whose components are ϕ_{ij}), one can easily show [12] that the second moments of the displacements u_i (Green's function coefficients G_{ij}) satisfy

$$\mathbf{G}_{ij} = \beta \langle u_i u_j \rangle = [\mathbf{\Phi}^{-1}]_{ij}. \tag{4}$$

The equivalent relation in reciprocal space is derived at the end of this section. Thus Eq. 4 provides a feasible way to accurately construct the $\mathbf{\Phi}$ matrix

provided that a sufficiently large number of independent observations of $\{u_i\}$ in thermal equilibrium are known.

For harmonic system, the integrand of the partition function $Z(\beta)$ is a high-dimensional Gaussian distribution. Integrating out individual degrees of freedom will leave the Boltzmann factor of the remaining terms in a Gaussian form

$$\int du_n e^{-\beta V} \propto e^{-\beta V'}, \tag{5}$$

where $V' = \frac{1}{2}\sum_{i \neq n, j \neq n} \tilde{\phi}_{ij} u_i u_j$ and $\tilde{\phi}_{ij} = \phi_{ij} - \phi_{in}\phi_{jn}/\phi_{nn}$. V' and $\tilde{\phi}_{ij}$ are the effective renormalized potential energy and spring constants, respectively. In this fashion, all degrees of freedom that do not couple directly to any *external* force can be eliminated. In the given context of a semi-infinite elastic solid in contact with an adsorbate or a substrate, it will be reasonable to assume that only the first layer interacts with the adsorbate and/or substrate, respectively. The effect of all other layers can be incorporated in the single Green's function layer.

The procedure described above to eliminate harmonic degrees of freedom applies to periodic and non-periodic systems alike. However, the method is better suited for periodic systems due to their translational invariance, which allows for a sparse representation of the effective interactions, i.e., instead of calculating the effective spring constants between individual surface atoms in real space, it is more efficient to assess them in reciprocal space. This is because modes with different wave vectors do not couple with each other in periodic systems with harmonic degrees of freedom. If $\mathbf{u}_n$ is the displacement vector of atom n with mean equilibrium position $\mathbf{R}_n^0$ in real space, its Fourier transform is defined as

$$\tilde{\mathbf{u}}(\mathbf{q}) = \frac{1}{\sqrt{N}}\sum_n \mathbf{u}_n \exp(-i\mathbf{q}\mathbf{R}_n^0). \tag{6}$$

The spring constant matrix in reciprocal space $\tilde{\boldsymbol{\Phi}}$ would be reconstructed according to Eq. 4 as

$$\tilde{\boldsymbol{\Phi}}_{\alpha\beta}(\mathbf{q}) = [\tilde{\mathbf{G}}^{-1}(\mathbf{q})]_{\alpha\beta}, \tag{7}$$

where the Green's function in reciprocal space reads

$$\tilde{\mathbf{G}}_{\alpha\beta}(\mathbf{q}) = \frac{1}{k_B T}\langle \tilde{\mathbf{u}}_\alpha(\mathbf{q})\tilde{\mathbf{u}}_\beta^*(\mathbf{q})\rangle. \tag{8}$$

Here "*" denotes the complex conjugate. Thus, for three-dimensional simple crystals with N atoms in the interface, one only has to acquire and diagonalize N matrices each having dimension 3×3, instead of accumulating and diagonalizing one large $3N \times 3N$ Green's function matrix.

Once the $\tilde{\boldsymbol{\Phi}}$ matrix has been obtained, the elastic force on atoms in the Green's

function layer can be readily obtained by

$$\tilde{\mathbf{f}}_\alpha(\mathbf{q}) = -\sum_\beta \tilde{\boldsymbol{\Phi}}_{\alpha\beta}(\mathbf{q})\tilde{\mathbf{u}}_\beta(\mathbf{q}),\tag{9}$$

where $\tilde{\mathbf{u}}_\alpha(\mathbf{q})$ is the α component of the displacement field expressed in reciprocal space defined in Eq. 6. By transforming $\tilde{\mathbf{f}}_\alpha(\mathbf{q})$ back into the real space, one will obtain the corresponding elastic force $\mathbf{f}(\mathbf{r})$ in real space.

While we do not consider deviations from perfect crystallinity here, we would like to mention that it will be possible to conduct simulations with local inhomogeneities by using Green's functions reflecting the long-wavelength behavior plus local perturbations, which would need to be augmented by local interactions. Algorithms have been developed for instance in the context of lattice cavities in Ref. [13].

In the remainder of this section, we will derive the fluctuation-dissipation relation which forms the basis for our approach. Consider a crystal in which the (effective) interaction potential between atoms is given by

$$V = \frac{1}{2}\sum_{n,n'}\sum_{\alpha,\alpha'}\Phi_{n,n'}^{\alpha,\alpha'}u_{n,\alpha}u_{n',\alpha'}.\tag{10}$$

Here n enumerates the elementary cells and α the Cartesian coordinates of the atoms contained in an elementary cell. For periodic systems, the (renormalized) force constants $\Phi_{n,n'}^{\alpha,\alpha'}$ only depend on the relative vector $\Delta\mathbf{R}_{n,n'}^0 = \mathbf{R}_n^0 - \mathbf{R}_{n'}^0$.

Using the definition of the Fourier transform in Eq. 6 for the displacements, one can substitute $u_{n\alpha}$ with $\sum_\mathbf{q}\tilde{u}_\alpha(\mathbf{q})\exp(i\mathbf{q}\mathbf{R}_n^0)/\sqrt{N}$ and thus,

$$V = \frac{1}{2N}\sum_{\mathbf{q},\mathbf{q}'}\sum_{\alpha,\alpha'}\tilde{u}_{\alpha'}^*(\mathbf{q}')\,\tilde{u}_\alpha(\mathbf{q})\underbrace{\sum_n e^{i(\mathbf{q}-\mathbf{q}')\mathbf{R}_n^0}}_{N\delta_{\mathbf{q},\mathbf{q}'}}\underbrace{\sum_{\Delta\mathbf{R}_{n,n'}^0}\Phi_{n,n'}^{\alpha,\alpha'}e^{-i\mathbf{q}'\Delta\mathbf{R}_{n,n'}^0}}_{\tilde{\Phi}_{\alpha\alpha'}(\mathbf{q}')}\tag{11}$$

$$= \frac{1}{2}\sum_\mathbf{q}\sum_{\alpha,\alpha'}\tilde{u}_\alpha(\mathbf{q})\tilde{\Phi}_{\alpha,\alpha'}(\mathbf{q})\tilde{u}_{\alpha'}^*(\mathbf{q}).\tag{12}$$

Inserting identities in the form of $\delta_{\alpha\beta} = \sum_\gamma U_{\alpha\gamma}U_{\gamma\beta}^*$, where the $U_{\alpha\gamma}$ is the $\alpha\gamma$ components of a unitary matrix, one can rewrite Eq. 12 as

$$V = \frac{1}{2}\sum_\mathbf{q}\underbrace{\tilde{u}_\beta(\mathbf{q})U_{\beta\gamma}}_{\hat{u}_\gamma(\mathbf{q})}\underbrace{U_{\gamma\alpha}^*\tilde{\Phi}_{\alpha\alpha'}(\mathbf{q})U_{\alpha'\gamma'}}_{\hat{\Phi}_{\gamma\gamma'}}\underbrace{U_{\gamma'\beta'}^*\tilde{u}_\alpha^*(\mathbf{q})}_{\hat{u}_{\gamma'}^*(\mathbf{q})}\tag{13}$$

where we have assumed the summation convention in Greek indices. Now assume that U represents the unitary transformation that diagonalizes the

6

$\tilde{\Phi}$ matrix so that the components of $\hat{\mathbf{u}}$ can be interpreted as independent eigenmodes. (This transformation exists because $\tilde{\Phi}$ is a symmetric positive definite matrix; $\tilde{\Phi}$ at Γ point is special, it may have zero eigenvalues but is still symmetric.) Consequently, the equipartition theorem applies for each component in $\hat{u}_\gamma$ and thus,

$$k_B T \left[\hat{\Phi}^{-1} \right]_{\alpha\alpha'} = \langle \hat{u}_\alpha(\mathbf{q}) \hat{u}_{\alpha'}^*(\mathbf{q}) \rangle \tag{14}$$

Setting $\hat{G}_{\alpha\alpha'} = \left[\hat{\Phi}^{-1} \right]_{\alpha\alpha'}$ and transforming back into the original coordinate system yields

$$\tilde{G}_{\alpha\alpha'} = \frac{1}{k_B T} \langle \tilde{u}_\alpha(\mathbf{q}) \tilde{u}_{\alpha'}^*(\mathbf{q}) \rangle . \tag{15}$$

Note that Eq. 15 differs from the related Eq. 13 in reference [4], where a typo was made by placing the complex conjugate sign over the first term on the right-hand side. The error seems irrelevant for systems without basis, however, when the index α runs over the Cartesian components of more than one atom, the difference becomes noticeable.

In practice, it is easier to measure absolute atomic positions rather than displacements. As is seen in Eq. 8, the measurement of the Green's functions requires the evaluation of the atomic displacement, $\tilde{u}_\alpha(\mathbf{q}) = \tilde{R}_\alpha(\mathbf{q}) - \tilde{R}_\alpha^0(\mathbf{q})$, where $\tilde{R}_\alpha(\mathbf{q})$ is the instantaneous position of surface atoms in the reciprocal space, and $\tilde{R}_\alpha^0(\mathbf{q})$ is the corresponding mean equilibrium position, which satisfies

$$\tilde{R}_\alpha^0(\mathbf{q}) = \langle \tilde{R}_\alpha(\mathbf{q}) \rangle. \tag{16}$$

Consequently, the Green's function in Eq. 8 could then be expanded as

$$\begin{aligned} \tilde{\mathbf{G}}_{\alpha,\beta}(\mathbf{q}) &= \langle \tilde{u}_\alpha(\mathbf{q}) \tilde{u}_\beta^*(\mathbf{q}) \rangle \\ &= \langle [\tilde{R}_\alpha(\mathbf{q}) - \tilde{R}_\alpha^0(\mathbf{q})][\tilde{R}_\beta(\mathbf{q}) - \tilde{R}_\beta^0(\mathbf{q})]^* \rangle \\ &= \langle \tilde{R}_\alpha(\mathbf{q}) \tilde{R}_\beta^*(\mathbf{q}) \rangle - \langle \tilde{R}_\alpha(\mathbf{q}) \rangle \tilde{R}_\beta^{0*}(\mathbf{q}) \\ &\quad - \tilde{R}_\alpha^0(\mathbf{q}) \langle \tilde{R}_\beta^*(\mathbf{q}) \rangle + \tilde{R}_\alpha^0(\mathbf{q}) \tilde{R}_\beta^{0*}(\mathbf{q}) \\ &= \langle \tilde{R}_\alpha(\mathbf{q}) \tilde{R}_\beta^*(\mathbf{q}) \rangle - \tilde{R}_\alpha^0(\mathbf{q}) \tilde{R}_\beta^{0*}(\mathbf{q}) \\ &= \langle \tilde{R}_\alpha(\mathbf{q}) \tilde{R}_\beta^*(\mathbf{q}) \rangle - \langle \tilde{R}_\alpha(\mathbf{q}) \rangle \langle \tilde{R}_\beta^*(\mathbf{q}) \rangle. \end{aligned} \tag{17}$$

Thus by replacing $\langle \tilde{u}_\alpha(\mathbf{q}) \tilde{u}_\beta^*(\mathbf{q}) \rangle$ with $\langle \tilde{R}_\alpha(\mathbf{q}) \tilde{R}_\beta^*(\mathbf{q}) \rangle - \langle \tilde{R}_\alpha(\mathbf{q}) \rangle \langle \tilde{R}_\beta^*(\mathbf{q}) \rangle$, the instantaneous positions are evaluated rather than the displacements. This also reduces roundoff errors, aided by the fact that $\langle \tilde{R}_\alpha(\mathbf{q}) \rangle$ is expected to be zero in equilibrium for $\mathbf{q} \neq 0$.

3 Notes on implementation and technical issues

In this section, a few technical issues will be discussed, which arose while implementing the GFMD method into the open source package LAMMPS [7–9]. The main points are related to (i) what procedure is done in which fix, (ii) how to deal with lattices with basis, (iii) how to deal with non-orthorhombic lattice, (iv) how to reduce finite-size and anharmonic effects, (v) and how to interpolate the stiffness coefficients from small systems to large systems.

3.1 FixGFC and FixGFMD

The measurement of effective elastic stiffness coefficients based on the fluctuation-dissipation theorem was realized in FixGFC. It takes the instantaneous positions of surface atoms in the equilibrated system, and transforms them into reciprocal space to get the Green's functions. After every given number of measurements, the elastic stiffness coefficients are calculated and written to a binary file as well as a text log file.

The FixGFMD, however, does the real job for Green's function molecular dynamics. It reproduces the effective elastic force on a single layer of atoms from the bulk material that has now be integrated out, by utilizing the effective elastic stiffness coefficients — either read from the binary file produced in FixGFC or calculated from the analytic solutions for simple cubic systems [10,11]. At each time step, it computes the displacements $\mathbf{u}(\mathbf{r})$ of all atoms in the manifold and transforms them into the reciprocal space yielding $\tilde{\mathbf{u}}(\mathbf{q})$, and multiplies $\tilde{\mathbf{u}}(\mathbf{q})$ by the $\tilde{\boldsymbol{\Phi}}$ matrix, the resultant elastic force in reciprocal space $\tilde{\mathbf{f}}(\mathbf{q})$ is then transformed back into the real space and added to the corresponding atoms in the manifold.

In both fixes, the Fourier transformations are realized by calling subroutines from FFTW 2.1.5 (http://www.fftw.org) The FFTW libraries are therefore required when compiling LAMMPS together with current extensions.

3.2 Lattices with basis

When dealing with a non-primitive lattice, i.e., a lattice with basis, one simply extends the indices α in $\mathbf{u}_\alpha$ (and therefore $\tilde{\mathbf{G}}_{\alpha\beta}$, $\tilde{\boldsymbol{\Phi}}_{\alpha\beta}$ and so on) to $k\alpha$, where k runs over all atoms in the unit cell. For a lattice with basis, one may be tempted to generalize the kernel of the Fourier transformation in Eq. 6 from $\exp(-i\mathbf{q}\mathbf{R}_n^0)$ to $\exp(-i\mathbf{q}\mathbf{R}_{n,k}^0)$, where $\mathbf{R}_{n,k}^0$ is the equilibrium position of the k'th atom in the n'th cell. Doing this would result in new transformation

8

matrices and new force constant matrices in reciprocal space, but yielding exactly the same elastic force during Green's function molecular dynamics. Consequently although this procedure is legitimate, it introduces unnecessary extra floating point operations during the execution of the code. We therefore recommend the kernel ussing $\exp(-i\mathbf{q}\mathbf{R}_n^0)$, as in Eq. 6.

3.3 Non-orthorhombic lattices

The use of non-orthorhombic lattices may invoke difficulties regarding periodic boundary conditions. As an example, consider a triclinic solid placed into an orthorhombic simulation cell, as shown in Fig. 1. As is clear from the figure, triclinic solids may lead to skewed periodic boundary conditions. As a consequence, one risks having inconsistent periodic-boundary conditions for the solid and its FFT representation.
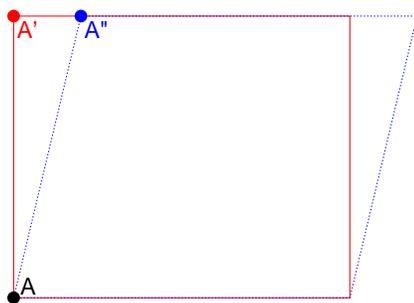
Fig. 1. (Color online.) Demonstration of potential difficulties associated with periodic boundary conditions. If the solid has a non-orthorhombic lattice (dotted, blue line) and is then placed into an orthorhombic simulation cell (solid, red line) in which the periodic boundary conditions are expressed in terms of that (red) cell, the periodicity of the FFT representation (same as the original non-orthorhombic (blue) lattice) would be different from the one imposed during MD (red orthorhombic cell).

Such inconsistency in periodicity would make the resultant elastic force incorrect during GFMD when an external force is applied to the GFMD manifold. For example, the periodicity of simulation box (the orthorhombic cell) would require that forces on atom A and its image A' be the same, while the FFT representation would require A and A'' to share the same force. As a result, the force on A' and A'' would be wrong, except in very special circumstances.

The solution to this problem is to simply adopt non-orthorhombic geometry for everything in the simulation (for example, by specifying a non-orthorhombic box when data is read in in LAMMPS) instead of placing it into an orthorhombic box. Thus the periodicity in the simulation cell and its FFT representation will be the same.

3.4 Finite size and anharmonic effects

The system size dependence of the measured elastic stiffness coefficients is another crucial issue that requires special attention. The finite size effect is mainly observed on effective elastic stiffness coefficients at the Γ-point, in that the eigenvalues corresponding to translational motions (acoustic eigenvalues) of the $\tilde{\boldsymbol{\Phi}}$ matrix at Γ (i.e., $\mathbf{q} = 0$) are of finite values instead of zero. Generally these finite values decrease as the system size increases. As a result, the finite size effect stiffens the measured $\tilde{\boldsymbol{\Phi}}(\Gamma)$.

Such "stiffening" is not expected since translational motions do not introduce internal interactions. To eliminate/reduce this finite size effect one could, of course, measure the effective elastic stiffness coefficients with a large enough simulation cell. However, it is neither efficient nor necessary. Instead, we prefer to adopt an alternative way that will reduce the finite size effect satisfactorily. First, the eigenvalues $\boldsymbol{\Lambda}$ and the corresponding eigenvectors $\mathbf{Q}$ of the measured $\tilde{\boldsymbol{\Phi}}(\Gamma)$ are computed. Second, the acoustic eigenvalues are set to zero (in practice, in order to avoid numerical problems, they are divided by 10^8 for systems with basis), while the remaining ones are kept untouched, yielding $\tilde{\boldsymbol{\Lambda}}$. Finally, the original $\tilde{\boldsymbol{\Phi}}(\Gamma)$ is replaced by $\tilde{\boldsymbol{\Phi}}' = \mathbf{Q}\tilde{\boldsymbol{\Lambda}}\mathbf{Q}^{-1}$. In effect, such treatment actually resets $\tilde{\boldsymbol{\Phi}}(\Gamma)$ to be zero for systems without a basis while modifies the elements of $\tilde{\boldsymbol{\Phi}}(\Gamma)$ slightly for system with a basis, making its acoustic eigenvalues close to zero, thus eliminating the finite size effect significantly.

Opposing the finite size effect, the anharmonic effect softens the measured $\tilde{\boldsymbol{\Phi}}$ at *all* $\mathbf{q}$ points. There is no general method, such as the rescaling used in eliminating finite size effects, to reduce the anharmonic effect. One could however reduce the temperature used in the measurement, making the system more "harmonic" to produce reliable effective stiffness coefficients.

3.5 Interpolation of stiffness coefficients to larger systems

Frequently, the size of the single layer used in GFMD is greater than that of the surface layer used in the stiffness coefficients measurement. It is therefore necessary to have some method to get the stiffness coefficients from the measured ones with a high precision. This is feasible since in reciprocal space, the $\boldsymbol{\Phi}$ matrix is continuous and periodic with a periodicity of $2\pi/\mathbf{a}$. Provided the simulation boxes share the same symmetry, $\boldsymbol{\Phi}$ does not depend on the system size other than the finite size effect discussed above — for larger system, one simply has a denser $\mathbf{q}$ mesh.

In our previous implementation [4], use of the phonon dispersion-like prop-

erties of the stiffness coefficients were made. Although this method works in most situations it may be unfeasible to get all the symmetry allowed coefficients for each given system, in particular when several atoms are contained in the basis. Instead, one would like to have an interpolation scheme. In this regard, the bicubic spline interpolation method is a good choice. However, one difficulty is that the stiffness coefficient can have a cusp. Noticing that the cusp always lies at $\mathbf{q} = 0$ in the reciprocal space, we adopted a mixed scheme to perform the interpolation: bi-linear interpolation is employed for points in the immediate vicinity of $\mathbf{q} = 0$, while bi-cubic interpolation is used for all other points where no cusp appears.

4 Applications

In this section, three test runs will be presented to demonstrate the validity and usage of the implemented fixes.

First, we take a simple cubic (2+1)-dimensional solid (we will integrate out the 1-dimension perpendicular to the interface leaving a 2-dimensional surface) as an example to measure its stiffness coefficients by FixGFC. While simple cubic solids are not very common in nature, they constitute good test systems as there is an analytical solution of the stiffness coefficients available. Saito[11] derived the exact Green's function for a simple cubic solids of lattice constant $a = 1$ (reduced units are used in this example, i.e., the units of length, mass, and energy are taken as unity) with nearest and second-nearest harmonic interaction

$$E = \frac{1}{2} \sum_{[i,j]} k_{ij} (r_{ij} - r_{ij}^0)^2, \tag{18}$$

where $k_{ij} = 1$, r_{ij}^0 equals 1 and $\sqrt{2}$ for nearest and second-nearest neighbor pair, respectively. $[i, j]$ runs over all nearest and second-nearest neighbor pairs. A simple cubic lattice with size $16 \times 16 \times 16$ was constructed, whose topmost layer was held fixed while the others were free to move. Periodic boundary condition was applied in the x and y (planar) directions. The system was then equilibrated at a temperature of 0.005 for 500,000 molecular dynamics steps. The time step was set to be 0.005. The Green's function of the bottom layer (surface atoms) was measured every 20 time steps during the following simulation procedure.

The diagonal components of the obtained stiffness coefficients along the major symmetry directions in the Brillouin zone are shown in Fig. 2. The analytic solution for a semi-infinite system by Saito[11] is also shown as lines. One observes that, first, the stiffness coefficients obtained are similar to phonon-dispersion curves. This is expected for a system without a basis. Secondly, because of the pure harmonic interactions, anharmonic effects are not observed.
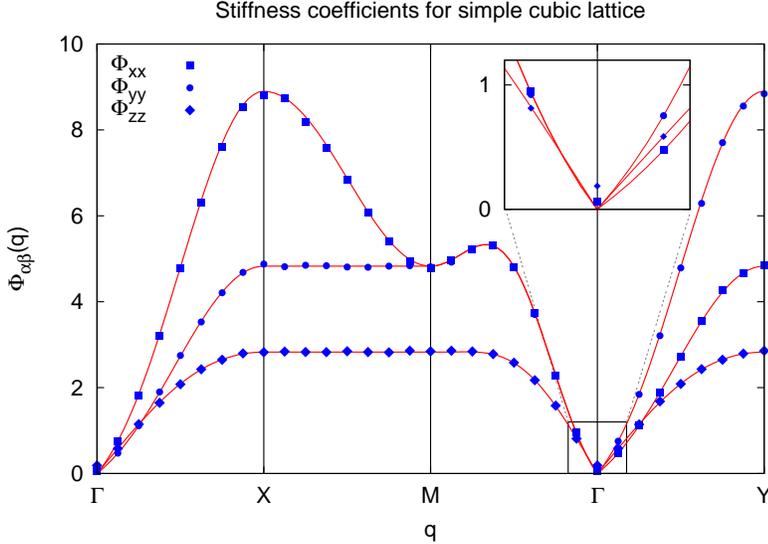
Fig. 2. Numerical (symbols) and analytical (Ref. [11], lines) results of the diagonal components of $\tilde{\mathbf{\Phi}}_{\alpha\beta}(\mathbf{q})$ for simple cubic crystal lattice along the major symmetry directions in the surface Brillouin zone. The inset shows a magnification of the vicinity of Γ-point.

However, finite-size effects are clearly seen. At the Γ point, the measured $\tilde{\Phi}_{\alpha\beta}$'s are of small but finite values, while the analytic solutions give exactly zero (see inset of Fig. 2). Thirdly, cusps are found for all diagonal components around the Γ-point. Last but not least, other than at the Γ point, the coefficients computed by FixGFC, based on the fluctuation-dissipation theorem, agree very well with the analytic ones. Similar agreement is also found in the off-diagonal components, which are not shown here. Such agreement confirms the feasibility of using the fluctuation-dissipation theorem to determine the stiffness coefficients, as well as the validity of the current implementation, FixGFC.

We now take a hexagonal lattice as another example to further illustrate the measurement of effective elastic stiffness coefficients, but for a (1+1) dimension system. Two models with sizes of 16×18 and 64×74, respectively, were constructed, as in the previous case, with the topmost layer (actually, it is a line of atoms for our (1+1)-dimensional system) fixed and the others free. The interaction between atoms was described by a Lennard-Jones potential

$$E = 4\epsilon \left[\left(\frac{\sigma}{r}\right)^{12} - \left(\frac{\sigma}{r}\right)^{6} \right], r < r_{\text{cutoff}} \tag{19}$$

with $\sigma = 1$, $\epsilon = 1$ cutoff at 2.5. Figure 3 shows the elastic stiffness coefficients obtained as a function of wave number $\mathbf{q}$. As expected the elastic stiffness coefficients have a periodicity of 2π in the reciprocal space. The elastic stiffness coefficients, other than at the Γ point, do not show notable size-dependence. The finite size effect is clearly seen for $\tilde{\mathbf{\Phi}}(\Gamma)$. However, after rescaling $\tilde{\mathbf{\Phi}}(\Gamma)$,

12
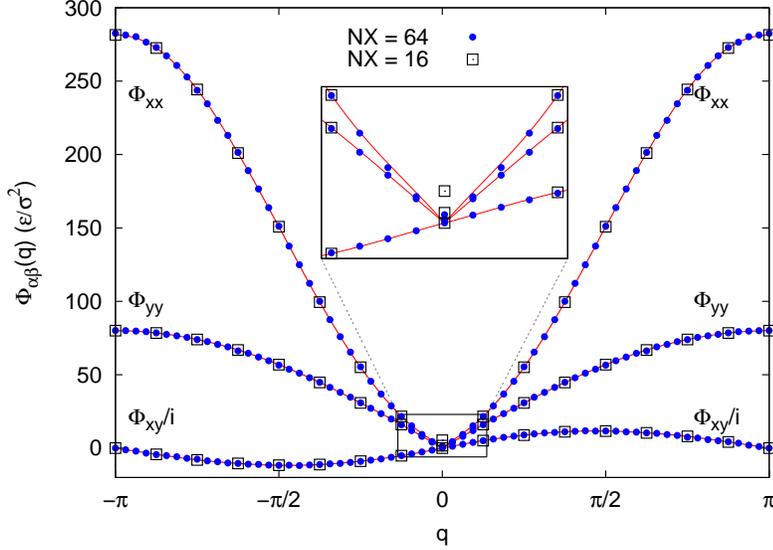
Fig. 3. Elastic stiffness coefficients for (1+1)-dimensional hexagonal lattice with Lennard-Jones interaction as a function of wave number q. Symbols are results computed by FixGFC for different system size; solid lines are results interpolated from those for system size of 16×18, after rescaling $\tilde{\mathbf{\Phi}}(\Gamma)$. The inset is a magnification of the vicinity of Γ-point.

the interpolated data do not show notable finite size effects. Such observations give confidence in the reliability of the interpolated elastic stiffness coefficients.

The charm of GFMD lies in its potential to model real materials. As a third example, we take the (111) surface of Cu to illustrate one of the possible applications of GFMD, namely the indentation of a surface against an indenter.

Twenty Cu(111) layers (39.7 Å in thickness) with surface dimension of 39.8×40.9 Å^2 (9×16 unit surface cells) were modeled to measure the elastic stiffness coefficients. This is a typical case whose unit surface cell has a basis with two atoms. A full atom molecular dynamics simulation was run at 300K based on an embedded-atom-method (EAM) potential [15] and the elastic stiffness coefficients were measured by FixGFC on the bottom layer. The diagonal components of the obtained elastic stiffness coefficients are shown in Fig. 4. Unlike the primitive cell cases shown above, the relation between the stiffness coefficients and $\mathbf{q}$ vectors do not show phonon-dispersion-like curves anymore. The corresponding component for each basis atom, e.g., $\tilde{\Phi}_{11}$ and $\tilde{\Phi}_{44}$, coincide with each other. This is expected, as both basis atoms are identical. The anharmonic effect is clearly seen here. In the whole reciprocal space, $\tilde{\mathbf{\Phi}}$'s measured at 300K are always smaller than those at 100K.

Secondly, another two Cu(111) models were constructed to simulate the indentation of a surface against a cylindrical indenter. The first one consists of 18×32 unit surface cells (79.7×81.8 Å^2) with only one layer, which is subjected to GFMD, by invoking FixGFMD, based on the elastic stiffness

13
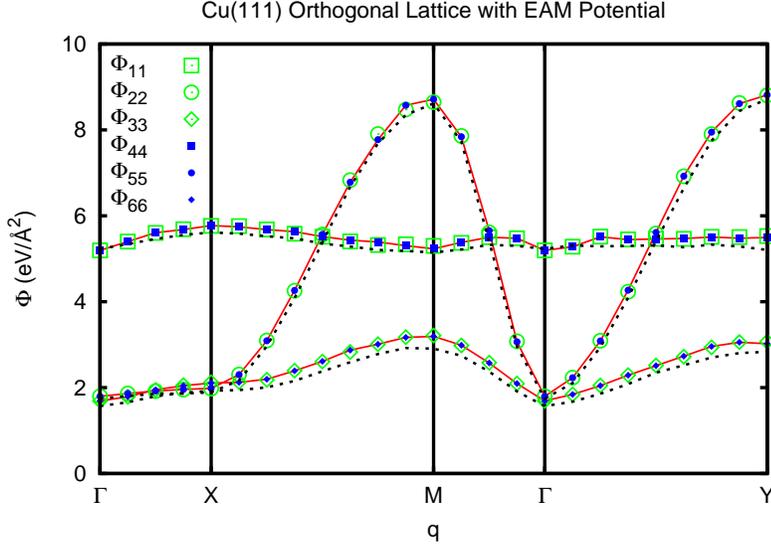
Fig. 4. Elastic stiffness coefficients based on embedded-atom-method potential for the (111) surface of FCC Cu with 2 atoms per unit surface cell, along the major symmetry directions in the Brillouin zone. Symbols and solid lines are results measured at 100K, while dotted lines are those measured at 300K.

coefficients obtained at 100K. The size of the surface layer is twice as long in both the x and y directions as that used in the FixGFC measurement, therefore interpolation of the elastic stiffness coefficients is necessary and performed. A cylindrical indenter was placed along the y direction underneath the surface layer, and an extra load of -0.01 eV/Å was applied to all atoms in the layer along the z direction. The second model consists of 18×32 unit surface cells with 40 layers in the z direction (81.4 Å in thickness). Full atom molecular dynamics simulation based on the EAM potential was carried out at 0K, with the same indenter placed and same amount of extra load applied to all atoms on the *topmost* layer (The extra load could also be added to the bottom layer, i.e., the layer that is in direct contact with the indenter. The same result would be obtained).

Fig. 5 compares the final positions of atoms in the layer that is in direct contact with the indenter as well as the normal pressure on these atoms exerted by the indenter from the full atom MD and GFMD. It is seen that both simulations agree quite well with each other, confirming that the GFMD can indeed reproduce the contact morphology/mechanics of the all-atom simulation.

Because of the coarse graining in the GFMD, the total number of atoms considered in the GFMD is significantly reduced — in the present case, 1/40 of the full-atom simulation. In turn, the total simulation time cost in GFMD is just about 2 seconds, while it is ~ 4300 seconds for full atom MD. The saving in computational cost is really amazing.

14

(a) Indentation shape

(b) $P_\perp$ exerted by the indenter
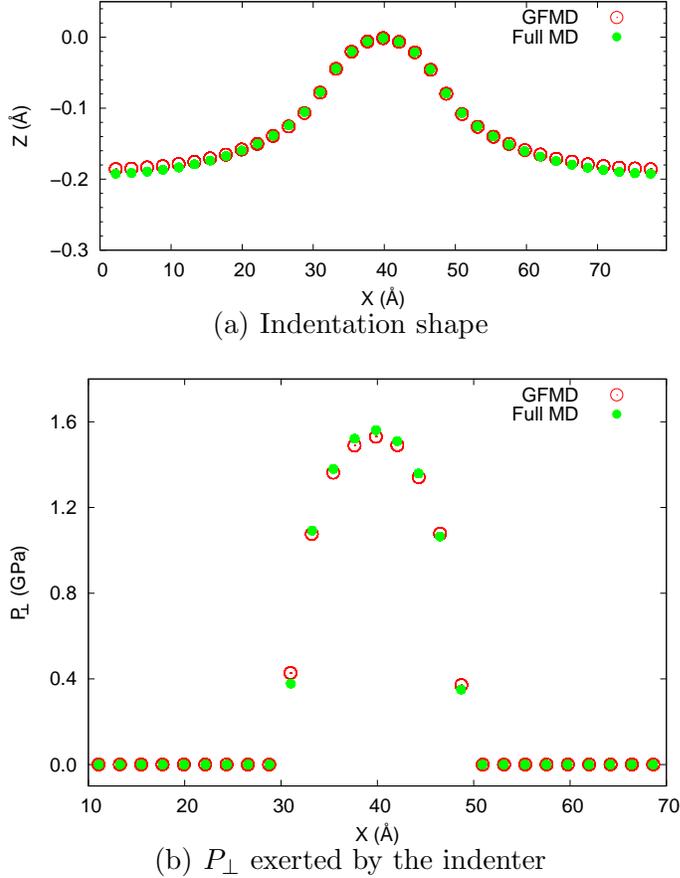
Fig. 5. Comparison of (a) the indentation shapes, (b) normal pressure exerted by the indenter, between full atom MD and Green's function MD for Cu(111) surface against a cylindrical indenter; view from the y direction. Only the bottom layer of the full-atom MD model is shown; the Z axis in (a) is enlarged by 100 times with respect to X for a better view.

5 Summary

In summary, we present in this paper an implementation of the Green's function molecular dynamics, as an extension to the existing open-source classical molecular dynamics code LAMMPS. It is demonstrated that the implementation is capable of evaluating the elastic stiffness coefficients precisely based on the fluctuation-dissipation theorem, and that the subsequent Green's function molecular dynamics based on the obtained elastic stiffness coefficients can reproduce perfectly the contact morphology of the all-atom simulation, while the computation time is reduced considerably. The implementation of GFMD

thus enables one to study the contact mechanics of a surface within the elastic deformation region with high precision as well as low computational costs.

References

[1] S. Hyun, L. Pei, J.-F. Molinari, and M. O. Robbins. Finite-element analysis of contact between elastic self-affine surfaces. *Phys. Rev. E*, 70(2):026117, Aug 2004.

[2] Shaobiao Cai and Bharat Bhushan. *Wear*, 259:1408–1423, 2005.

[3] C. Yang, U. Tartaglino, and B. N. J. Persson. A multiscale molecular dynamics approach to contact mechanics. *Eur. Phys. J. E*, 19:47–58, 2006.

[4] Carlos Campañá and Martin H. Müser. Practical Green's function approach to the simulation of elastic semi-infinite solids. *Physical Review B (Condensed Matter and Materials Physics)*, 74(7):075420, 2006.

[5] Carlos Campañá, Martin H. Müser, Colin Denniston, Yue Qi, and Thomas A. Perry. Elucidating the contact mechanics of aluminum silicon surfaces with green's function molecular dynamics. *Journal of Applied Physics*, 102(11):113511, 2007.

[6] R Kubo. *Rep. Prog. Phys.*, 29:255–284, 1966.

[7] S. J. Plimpton. Fast parallel algorithms for short-range molecular dynamics. *J. Comp. Phys.*, 117:1–19, 1995.

[8] S. J. Plimpton, R. Pollock, and M. Stevens. Particle-mesh ewald and rrespa for parallel molecular dynamics simulation. In *Proc of the Eighth SIAM Conference on Parallel Processing for Scientific Computing*, Minneapolis, MN, 1997.

[9] Large-scale Atomic/Molecular Massively Parallel Simulator, LAMMPS, available at: http://lammps.sandia.gov.

[10] Hideaki Uemura, Yukio Saito, and Makio Uwaha. Equilibrium morphology in two-dimensional heteroepitaxy on an elastic substrate. *Journal of the Physical Society of Japan*, 72(11):2856–2865, 2003.

[11] Yukio Saito. Elastic lattice Green's function in three dimensions. *Journal of the Physical Society of Japan*, 73(7):1816–1826, 2004.

[12] See for example, R. Kubo, M. Toda, and N. Hashitsume. *Statistical Physics II. Nonequilibrium Statistical Mechanics*. Springer, 2nd edition, 1991.

[13] J. Schiøtz and A. E. Carlsson. Calculation of elastic Green's functions for lattices with cavities. *Phys. Rev. B*, 56(5):2292–2294, Aug 1997.

[14] M. Parrinello and A. Rahman. Strain fluctuations and elastic constants. *The Journal of Chemical Physics*, 76(5):2662–2666, 1982.

[15] S. M. Foiles, M. I. Baskes, and M. S. Daw. *Phys. Rev. B*, 33:7983, 1986.